Core/shell Nanostructures Embedded in Solid

V. R. Radmilović[1,2]

[1]University of Belgrade, Faculty of Technology and Metallurgy, Nanotechnology and Functional Materials Laboratory, 11120 Belgrade, Serbia.
[2]National Center for Electron Microscopy, Lawrence Berkeley National Laboratory, Berkeley, CA 94720, USA.

VRRadmilovic@tmf.bg.ac.rs; VRRadmilovic@lbl.gov

Keywords: aberration-corrected HRTEM, core/shell nanostructures, light element imaging.

This study illustrates the importance of understanding the fundamental features that underlie the behavior of nanoscale phases with coherent interfaces embedded in a solid and their role in the evolution of microstructure in materials. The fundamental principles established using model systems are employed in the design and testing of new materials such as systems for energy-related applications. Key requirements for advanced alloys are high strength, light weight, coarsening resistance, corrosion resistance, high temperature stability, etc. Unfortunately, these requirements are mutually exclusive in many Al-based alloys. The extraordinary effects on mechanical properties arising from the formation of second-phase particles are well known, and exploited in applications ranging from energy generation to aerospace structures [1].

Al-Li and Al-Sc alloys are of great interest for aerospace and cryogenic applications due to their low density and high strength-to-weight ratio. The excellent mechanical properties of these alloys are based on a fine dispersion of coherent Al_3Li metastable and Al_3Sc stable precipitates. The aim of this report is to show the effect of Li addition on core/shell precipitate formation in the ternary Al-Li-Sc alloys. The atomic structure of these precipitates has been studied by a range of advanced microscopy techniques, such as high resolution TEM with exit wave reconstruction, atomic resolution HAADF imaging, and energy filtered electron energy loss spectroscopy (EELS), combined with the first principle calculation and continuum thermodynamic modeling to uncover the role of Li. We demonstrated that monodisperse Al_3LiSc core/shell ordered precipitates with a Sc and Li-rich core surrounded by a Li-rich shell can be created via a two-stage heat treatment. During the first aging stage at 450°C, Li incorporation into the cores leads to a burst of nucleation followed by rapid depletion of Sc solute. In the second stage, at 190°C, $Al_3(LiSc)$ cores become spherical substrates for solid-state epitaxial growth of Al_3Li, which leads to shell formation through a barrier-less process of solid state wetting [2]. The thickness of the core and shell are anti-correlated, such that the size distribution of the total core-shell particle is narrower than that of either the core or the shell. Li-rich shell shows almost no compositional differences between adjacent columns. By contrast, the core superlattice columns are highly disordered, evidence for random mixing of Li and Sc on these sites. The columns surrounding the superlattice columns are very uniform, showing the amount of solute atoms occupying these sites to be negligible. In fact, no anti phase boundary (APB) defects were observed in any of the investigated $Al_3(LiSc)$ core/shell precipitates. These defects are known to be very energy-costly at room temperature, i.e. 290 mJ/m^2 in Al_3Sc [3] and 118 mJ/m^2 in Al_3Li [4]. The first principle calculation predicts that the core-shell precipitates in the investigated AlLiSc alloy to be thermodynamically stable phases, with no driving force for the diffusion of Li out of the core into the shell. High-resolution phase contrast imaging and geometric phase analysis shown in Figure 1a and b, respectively, reveal that both, the core and the shell are fully ordered in the $L1_2$ structure and fully coherent with the surrounding fcc matrix. With prolonged aging time, for more than 1000h at 190°C, these particles exhibit coarsening, and create an interfacial dislocation at the Al_3Li shell/Al matrix interface, in order to accommodate coherent strain increase due to misfit in their lattice parameters, as shown in Figure 2a and b. Aberration corrected transmission electron microscopy was employed to image Li using exit wave reconstruction [5]. The phase of the exit wave shown in Figure 3 distinguished clearly Al columns from Li columns in the Li rich $L1_2$ shell [6]. Li concentration in the core could be calculated from scanning transmission electron microscopy of $Al_3(LiSc)$ nanoparticles. This procedure uses an analysis technique that normalizes the signal from the $L1_2$ superlattice columns to the immediately adjacent pure Al columns. By knowing that the total amount of Sc and Li is 25 at.%, the composition of each column can be determined individually. This calculation shows appreciable and uniform incorporation of 9.7 $\pm$ 2.4 at.% Li in the core of the precipitates. For this ternary AlLiSc alloy we show a way of producing an uniform distribution of coarsening resistant monodispersed $Al_3(LiSc)$ core/shell particles in an Al matrix with unusually narrow size distribution. A detailed analysis of these precipitates has provided important insights into their atomic structure and composition [7].

1. K. Lu, Science 328 (2010) 319.
2. V. Radmilović et al., Nature Materials 10 (2011) 710.
3. K. Fukunaga et al., Materials Science and Engineering A239–240 (1997) 202.
4. S.M. Jeon and J.K. Park, Acta Materialia 44 (1996)1449.
5. Y. Shao-Horn et al., Nature Materials 2 (2003) 464.
6. M. Rossell et al., Physical Review B 80 (2009) 024110.

7. I would like to thank to my former graduate students, post-docs and colleagues at The National Center for Electron Microscopy at Berkeley and at The University of Belgrade, Serbia, for their contributions to this project. This research is supported by the Department of Energy under contract no. DE-AC02-05CH11231. Supports of Nanotechnology and Functional Materials Center, funded by the European FP7 project No. 245916, and from the Ministry of Education and Science of the Republic of Serbia (project No. 172054), are also acknowledged.

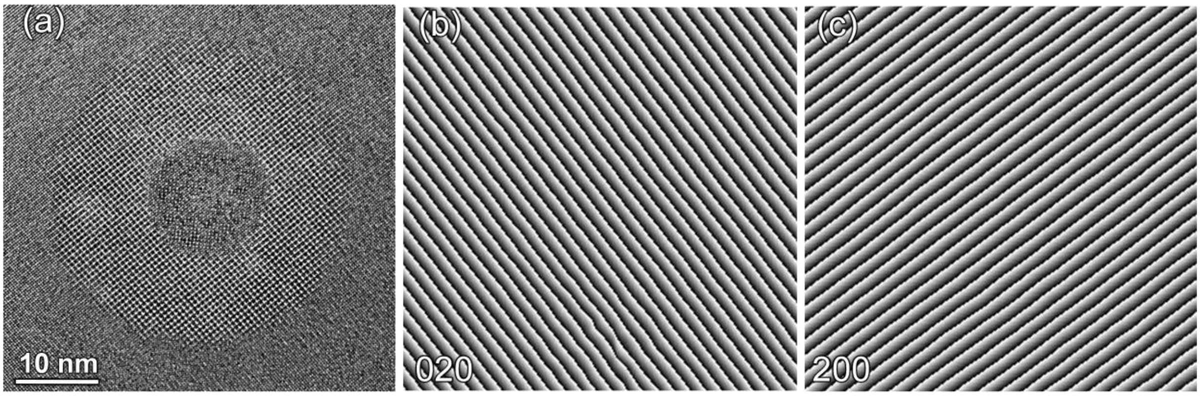

Figure 1. (a) HRTEM micrograph of a single $Al_3(LiSc)$ core-shell precipitate obtained at peak aging, after 4h at 190°C; (b) and c) Moire images created using 020 and 200 reflections in digital diffractogram, respectively, showing perfect alignment of {200} planes in both, Al matrix and core/shell precipitate; no dislocations at Al_3Li shell/Al matrix interface are present.

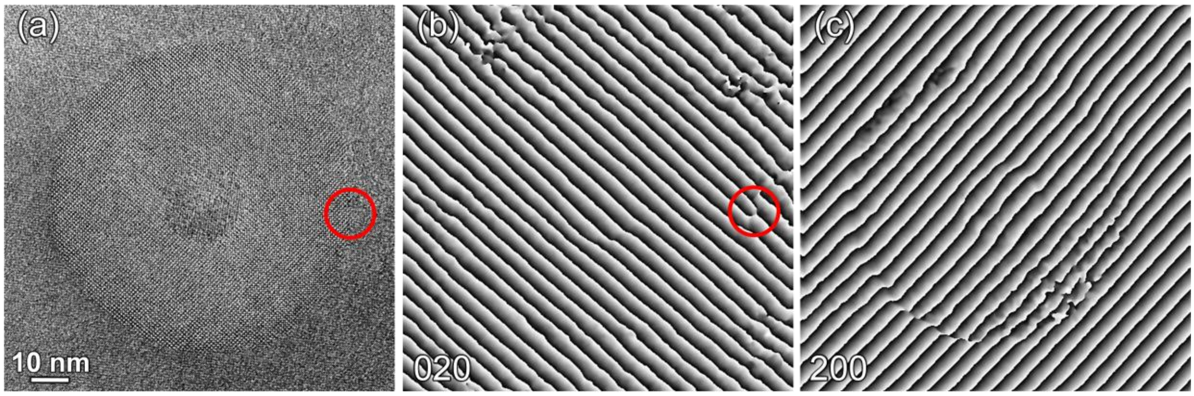

Figure 2. (a) HRTEM micrograph of a single $Al_3(LiSc)$ core-shell precipitate obtained from overaged sample, after 1000h at 190°C; (b) and (c) Moire images created using 020 and 200 reflections in digital diffractogram, respectively, showing significant distortion of {200} planes and the presence of dislocation at the Al_3Li shell/Al matrix interface (in the red circle).

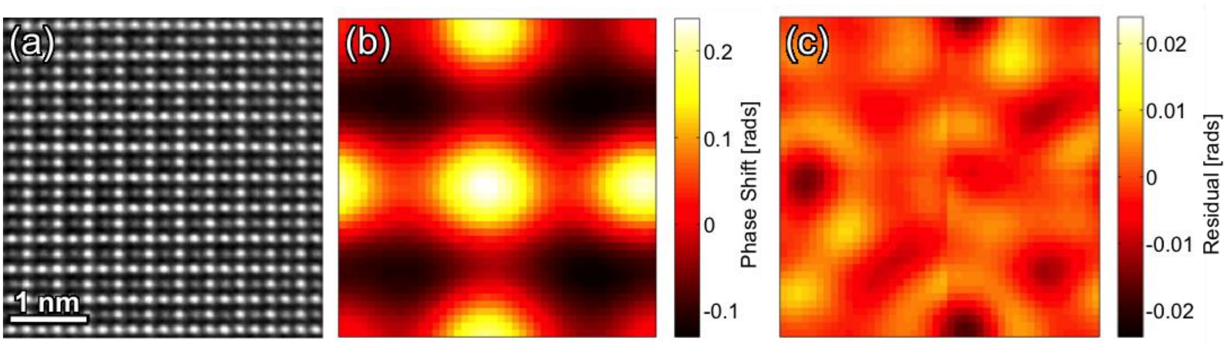

Figure 3. (a) Experimental high resolution exit wave phase image of Al_3Li ordered structure taken close to [001] zone axis; white dots are from Al columns and gray dots are from Li columns; (b) and (c) are 2D representation of the statistics of the experimental data, shown as the average experimental unit cell and the standard deviation image.